Am J Transl Res 2025;17(10):8407-8420
www.ajtr.org /ISSN:1943-8141/AJTR0167735

*Original Article*

# Multi-target mechanism of 6-O-Caffeoylarbutin in hyperuricemia treatment through *in vivo* validation and network pharmacology

Yang Zhang[1,2], Fanyi He[3], Kongchun Sun[1], Xuezhi Yu[1], Xiuzhen Chen[1], Li Zhou[2], Sheng Liu[2], Baochun Shen[1]

[1]*School of Pharmaceutical Sciences and Yunnan Provincial Key Laboratory of Pharmacology for Natural Products, Kunming Medical University, Kunming 650500, Yunnan, China;* [2]*Department of Pharmacy, The Third People's Hospital of Yunnan Province, Kunming 650011, Yunnan, China;* [3]*Department of Public Laboratory, The Third People's Hospital of Kunming City, Infectious Disease Clinical Medical Center of Yunnan Province, Kunming 650041, Yunnan, China*

Received July 28, 2025; Accepted October 21, 2025; Epub October 25, 2025; Published October 30, 2025

**Abstract:** Objective: To evaluate the therapeutic effects of 6-O-Caffeoylarbutin on hyperuricemia (HUA) and renal inflammation in a mouse model and explore its underlying multi-target mechanisms. Methods: A HUA mouse model was established using potassium oxonate and hypoxanthine. Mice were treated with 6-O-Caffeoylarbutin (100, 200, 300 mg/kg) or benzbromarone (10 mg/kg) for 14 days. Serum uric acid (SUA), creatinine, and xanthine oxidase (XOD) levels were measured. Renal injury and inflammation were assessed by H&E staining and ELISA for IL-1β, TNF-α, and IL-6. Network pharmacology and molecular docking predicted potential targets, which were validated by western blotting (WB). Results: Both 6-O-Caffeoylarbutin and benzbromarone significantly reduced renal tissue damage, tubular dilation, and interstitial edema by routine histology. In HUA mice, they also lowered SUA levels. ELISA showed significant reductions in IL-1β, TNF-α, and IL-6, indicating anti-inflammatory effects. Notably, the high-dose 6-O-Caffeoylarbutin group showed results comparable to benzbromarone. Network pharmacology identified six putative targets related to uric acid metabolism and inflammation, with molecular docking confirming stable binding. WB confirmed regulatory activity, showing reduced expression of XDH, SERPINE1, ALB, SLC37A4, SLC28A2, and HPRT1. Conclusion: 6-O-Caffeoylarbutin effectively reduces uric acid levels and alleviates renal inflammation in HUA mice through multi-target mechanisms, including inhibition of urate production, promotion of excretion, and anti-inflammatory activity. It shows promise as a natural therapeutic candidate for HUA.

**Keywords:** 6-O-Caffeoylarbutin, HUA, uric acid metabolism, inflammation, network pharmacology

## Introduction

Hyperuricemia (HUA) is a metabolic disorder characterized by elevated serum uric acid (SUA) levels, which can lead to hypertension, cardiovascular disease (CVD), diabetes mellitus, chronic kidney disease (CKD), and other nephropathies [1, 2]. It is primarily caused by dysregulation of purine metabolism or excessive consumption of high-purine foods such as red meat, seafood, and alcohol [3].

With dietary changes and modern lifestyle shifts, the prevalence of HUA exceeds 20% in Southeast Asia [4]. Although febuxostat and allopurinol, widely used in clinical practice, offer benefits, prolonged treatment can lead to adverse effects, including hepatotoxicity and hypersensitivity reactions [5]. Most current uric acid-lowering medications work by promoting uric acid excretion or inhibiting xanthine oxidase (XOD) activity. However, long-term use of these drugs may result in side effects, such as hepatotoxicity and allergic responses, limiting their broader use [6].

6-O-Caffeoylarbutin, derived from Arctostaphylos uva-ursi and Vaccinium myrtillus, is a compound linking 3,4-dihydroxycinnamic acid to hydroquinone-β-D-glucopyranoside [7]. It exhibits various biological activities, including radical scavenging, inflammation modulation,

https://doi.org/10.62347/OKLY4393

and metabolic pathway regulation [8]. Pretreatment with 6-O-Caffeoylarbutin significantly enhances antioxidant enzyme activity in serum and liver tissue and mitigates histologic damage and inflammation [9].

Human HUA is primarily driven by XOD activity [6], and 6-O-Caffeoylarbutin has been shown to boost antioxidant activity. Current research suggests that 6-O-Caffeoylarbutin may help maintain uric acid homeostasis. By inhibiting uric acid synthesis and promoting its excretion, it can reduce SUA levels and alleviate HUA and associated metabolic disorders. Inhibiting XOD decreases uric acid production, while regulating uric acid transporters (including URAT1, GLUT9, ABCG2) promotes the intestinal and renal excretion of uric acid, reducing its accumulation in the body. Additionally, 6-O-Caffeoylarbutin may protect the kidneys from damage caused by HUA by reducing oxidative stress and inflammation. By modulating NF-κB and MAPK signaling pathways, it decreases proinflammatory factors (IL-1β, TNF-α, and IL-6), thereby reducing uric acid-induced damage to the kidneys and other tissues. These findings indicate that 6-O-Caffeoylarbutin has potential as a natural uric acid-lowering agent giving protective effects through a multi-target mechanism [9, 10].

Given these properties, 6-O-Caffeoylarbutin may serve as a therapeutic option for HUA, also known as increased SUA levels. In this study, a mouse model was used to evaluate the therapeutic effects of 6-O-Caffeoylarbutin on inflammatory markers, renal function, and SUA levels. Western blotting (WB) was employed to validate the mechanism of action, following the identification of putative drug targets using network pharmacology and molecular docking techniques. This research aims to provide a theoretical foundation for developing novel natural uric acid-lowering therapies and to uncover the molecular mechanisms behind 6-O-Caffeoylarbutin's multi-target regulation of HUA.

## Materials and methods

### *Animals*

SPF male ICR mice (5 weeks old, weighing 25.0-30.0 g) in good health were used. The mice were housed under controlled conditions with a 12-hour light-dark cycle, a temperature range of 24-26°C, and a relative humidity of 40%-60%. All food, water, wood chips, and cages were autoclave sterilized before use. The animal experiments were approved by the Ethics Committee of Kunming Medical University, following the ethical guidelines for experimental animals (approval number: kmmu20240343). Euthanasia was performed using carbon dioxide after reaching the humane endpoint, ensuring ethical compliance.

### *HUA model establishment and biochemical analysis*

HUA was induced in male ICR mice by intraperitoneal injection of the uricase inhibitor potassium oxonate (PO) (300 mg/kg), combined with oral gavage of the uric acid precursor hypoxanthine (HX) (500 mg/kg), with a dosage volume of 0.1 mL/10 g body weight [11]. Approximately 72 hours after the final administration of PO and hypoxanthine (HX) for model induction, a small blood sample (~50 μL) was collected from the tail vein of a randomly selected subset of mice. Serum was separated by centrifugation, and SUA levels were quantified using an automatic biochemical analyzer (Beckman Coulter AU480). Mice showing a significant elevation in SUA levels compared to the normal control group were considered to have successfully developed HUA. The model mice were then randomly assigned to five groups (n = 6 per group), which included three 6-O-Caffeoylarbutin treatment groups (100 mg/kg, 200 mg/kg, and 300 mg/kg), the model group, the positive control group (benzbromarone, 10 mg/kg), and the normal control group. Drug interventions were administered by oral gavage for 14 consecutive days [12]. During the experiment, blood samples were collected from the tail vein of a randomly selected subset of mice. At the end of the experiment, terminal blood samples were taken after euthanasia, before tissue harvest. The blood samples were allowed to stay at room temperature for one hour, then centrifuged at 4°C for 10 minutes at 6500 rpm to extract serum.

### *H&E staining*

H&E staining was performed on kidney sections from each experimental group to assess renal tissue integrity and pathologic changes in hyperuricemic mice. Sections were stained

with hematoxylin for five minutes, differentiated in 1% acid alcohol, and blued in 0.2% ammonia water. They were then cleaned in xylene, counterstained with eosin for two minutes, dehydrated in graded ethanol, and mounted with permanent mounting media [13]. Kidney slides were examined using an Olympus BX53 light microscope. A blinded histopathologic assessment was performed by two independent pathologists. The following scoring system was applied:

Tubular Dilation: 0 = absent, 1 = mild (< 25% cortex involved), 2 = moderate (25-50% involved), 3 = severe (> 50% involved).

Interstitial Edema: 0 = absent, 1 = mild (focal separation of tubules), 2 = moderate (multifocal areas with clear separation), 3 = severe (extensive diffuse separation).

The scores from both observers were averaged to calculate a mean histopathologic injury score for each sample.

*Enzyme-linked immunosorbent assay (ELISA) analysis*

ELISA kits were used to measure serum levels of inflammatory markers: IL-1β, TNF-α, and IL-6 (Shanghai Yazyme Biotechnology Co., Ltd., China). Concentrations were determined following the manufacturer's protocols using commercially available kits. The effect of 6-O-Caffeoylarbutin on these inflammatory markers in hyperuricemic mice was evaluated through statistical comparisons. Additionally, the effects of 6-O-Caffeoylarbutin on HUA and inflammation were assessed using ELISA to measure the levels of Interleukin-1β (IL-1β), Tumor Necrosis Factor-α (TNF-α), and Interleukin-6 (IL-6) [14].

*Target prediction and pathway enrichment analysis of 6-O-Caffeoylarbutin in HUN treatment*

The SEA, SuperPred, and Swiss Target Prediction databases were used to predict potential targets of 6-O-Caffeoylarbutin based on its Canonical SMILES format, which was obtained from PubChem (https://pubchem.ncbi.nlm.nih.gov/). HUA-related genes (HUA-RGs) and urate nephropathy-related genes (UN-RGs) were extracted from ClinVar [15], DisGeNET [16], MalaCards [17], and Phenolyzer [18] databases to identify genes associated with the disease. Potential therapeutic targets for 6-O-Caffeoylarbutin were identified as the overlapping targets between genes related to the disease and those predicted by the chemical. Gene Ontology (GO) and Kyoto Encyclopedia of Genes and Genomes (KEGG) pathway enrichment analyses were performed using the ClusterProfiler package [19] in R, with a significance threshold set at $P < 0.05$ to explore the biological relevance of these targets.

*Construction of protein-protein interaction (PPI) network for candidate genes*

The intersected targets were uploaded to the STRING database, a platform for protein data retrieval, interaction prediction, and Cytoscape visualization. The count package in R was used to visualize and analyze the frequency of target interactions.

*Molecular docking of 6-O-Caffeoylarbutin with target molecules*

Using PyMol2.5.7, the protein 3D model was pre-processed by removing extra complexes and water molecules, and then saved in PDB format. Molecular docking was performed with AutoDockTools-1.5.7, and PyMol2.5.7 was used to map the binding sites and visualize the docking results. UniProt was used to locate the matching sequences for glucose-6-phosphate transporter (SLC37A4) and nucleoside transporter (SLC28A2), which were then imported into SWISS-MODEL [20] for homology modeling. The model was validated using SAVESv6.0 [21]. For other proteins, including albumin (ALB, PDB ID: 7FFR), HX phosphoribosyltransferase (HPRT1, PDB ID: 1Z7G), xanthine dehydrogenase (XDH, PDB ID: 2E1Q), and plasma serine protease inhibitor (SERPINE1, PDB ID: 7AQF), PDB IDs were used for structural analysis.

*Western blot (WB) analysis*

Approximately 100 mg of kidney tissue was homogenized in RIPA buffer (HMQWL, Sparkjade, China) using a grinder (KZ-5F-3D, Servicebio, China). After adding loading buffer (037,817,000, Epizyme, China), the homogenate was centrifuged, and the supernatant was heated for 10 minutes. Samples were then

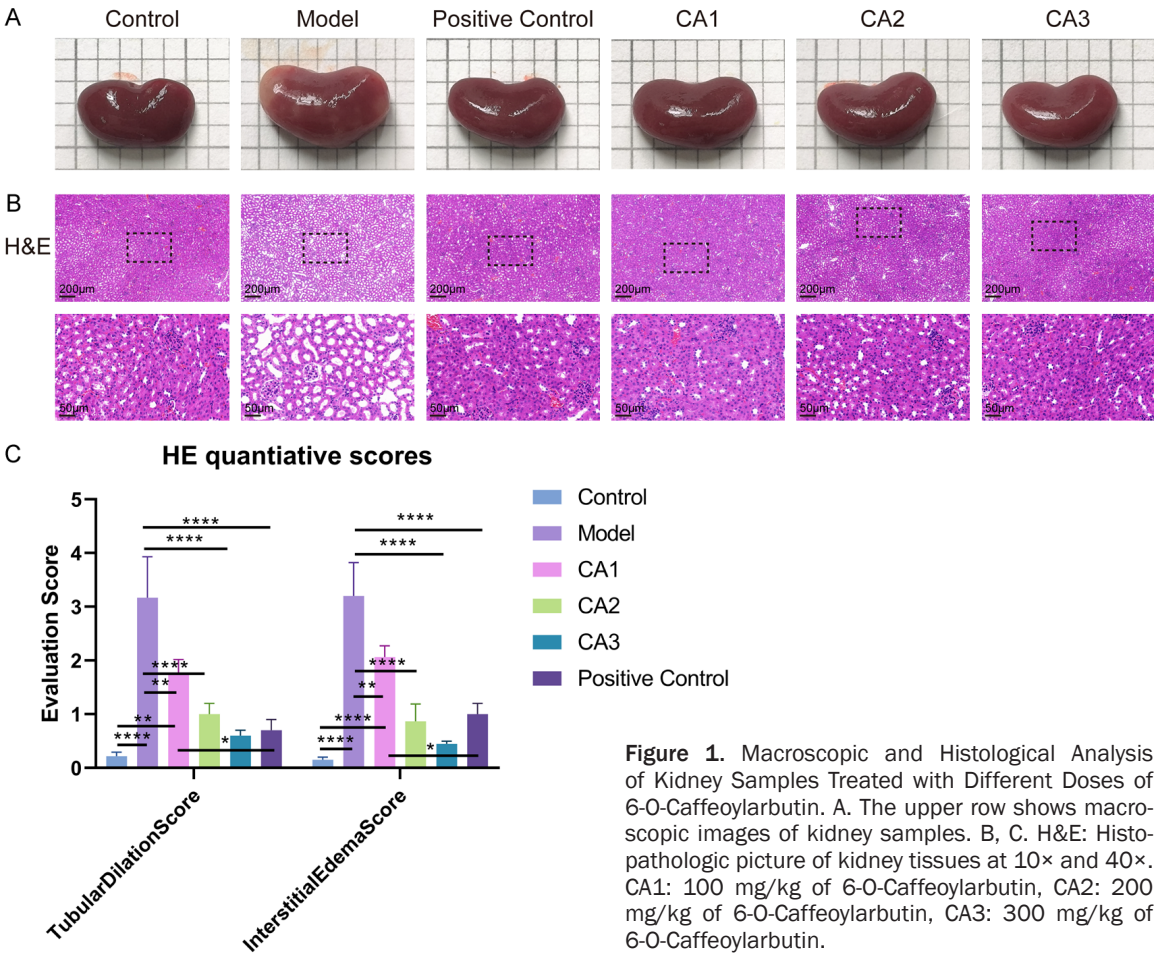


**Figure 1.** Macroscopic and Histological Analysis of Kidney Samples Treated with Different Doses of 6-O-Caffeoylarbutin. A. The upper row shows macroscopic images of kidney samples. B, C. H&E: Histopathologic picture of kidney tissues at 10× and 40×. CA1: 100 mg/kg of 6-O-Caffeoylarbutin, CA2: 200 mg/kg of 6-O-Caffeoylarbutin, CA3: 300 mg/kg of 6-O-Caffeoylarbutin.

electrophoresed on a 10% polyacrylamide gel and transferred to a PVDF membrane (000,203,376, Millipore). Membranes were blocked with BSA solution, incubated with primary antibodies (Anti-EGFR, 1:1000, Rabbit pAb, Wanleibio, cat# WL0682a, China; Anti-GAPDH, 1:5000, Mouse mAb, Proteintech, cat# 10,494-1-AP, China), followed by incubation with secondary antibodies. Other primary antibodies included Rabbit monoclonal anti-p-STAT3 (1:1000, Cell Signaling Technology, cat# 9145, United States) and Mouse monoclonal anti-STAT3 (1:1000, Cell Signaling Technology, cat# 9139, China). The secondary HRP-conjugated antibody (A0208, Beyotime, China) was used for detection. Protein bands were visualized using an enhanced chemiluminescence kit (KF003, Affinity, China) and analyzed with a Tanon 5200Multi chemiluminescence analyzer (China). Primary antibodies were diluted in TBST (Sparkjade, China).

*Statistical analysis*

Experimental data were analyzed using GraphPad Prism 9.0 software (GraphPad, San Diego, CA, USA). Comparisons between two groups were performed using a t-test, and comparisons among multiple groups were performed using one-way ANOVA, followed by Tukey's post hoc test for pairwise comparisons. Results are expressed as mean ± standard deviation (SD). A *P*-value of $< 0.05$ was considered significant.

## Results

*Effect of 6-O-Caffeoylarbutin on HUA*

Following the establishment of the HUA mouse model, significant renal tubular lumen dilation, color changes, and loss of renal tissue integrity were observed (**Figure 1A**). In the 6-O-Caffeoylarbutin (CA) treatment groups

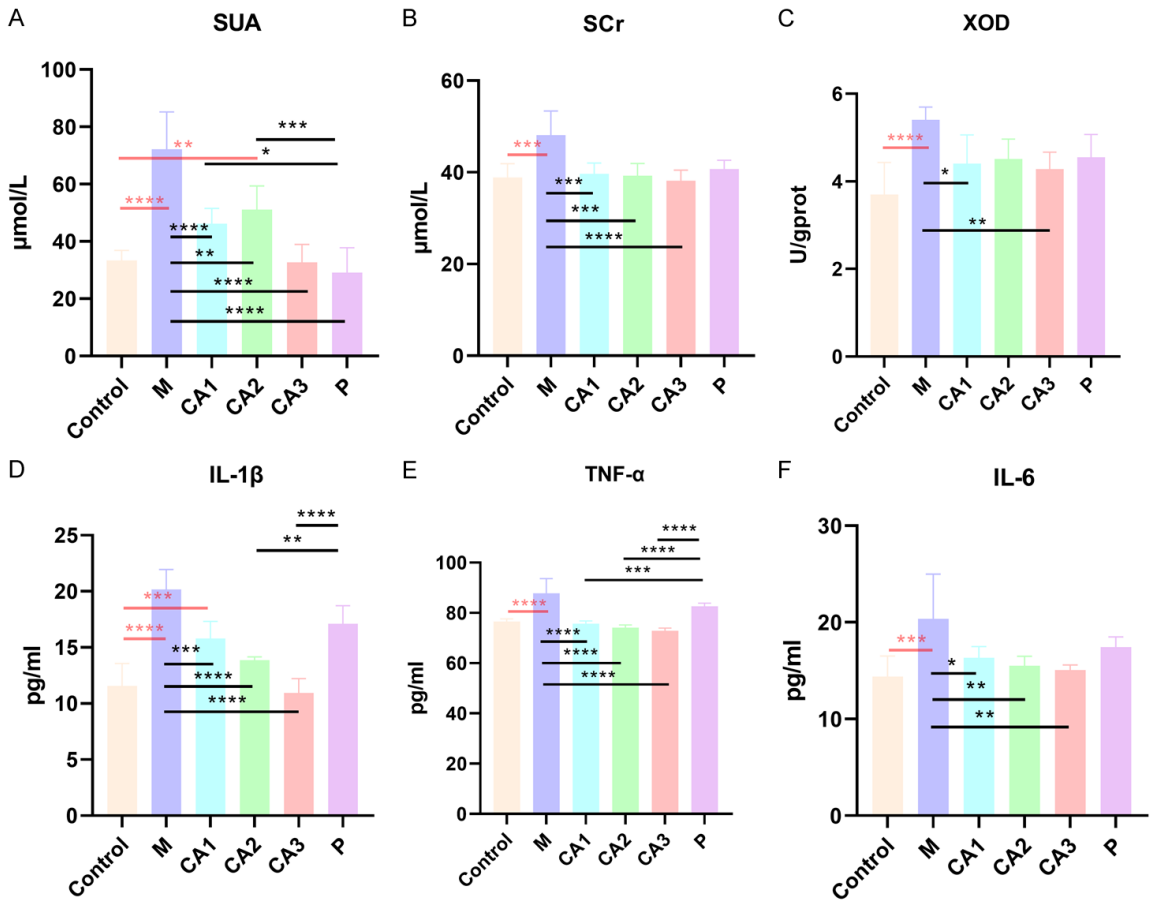


**Figure 2.** The bar graph shows the levels of various biochemical indicaors in the different experimental groups. Parameters (A-C) represent Serum Uric Acid (SUA), Serum Creatinine (SCr) and Xanthine Oxidase (XOD), respectively. Inflammatory factors (D-F) represent IL-1β, TNF-α and IL-6, respectively. Significance was determined by one-way ANOVA followed by Tukey's test. *P < 0.05, **P < 0.01, ***P < 0.001.

(CA1, CA2, and CA3), the renal tubular lumen appeared round or irregular, with less dilation and improved renal tissue integrity, reduced interstitial edema, and less neutrophil infiltration compared to the model group (**Figure 1B**). These preliminary observations were confirmed by quantitative analysis. Histopathological scores in the model group were significantly higher than those of the normal control group. Treatment with 6-O-Caffeoylarbutin reduced these scores in a dose-dependent manner, with the medium (CA2) and high (CA3) doses showing the most pronounced improvements in renal tissue injury. Additionally, the positive control group also demonstrated significant reductions in injury scores (**Figure 1C**).

Furthermore, we examined the levels of several inflammatory markers (IL-1β, TNF-α, and IL-6) in renal tissue. XOD, the key enzyme responsible for uric acid production, along with SUA and serum creatinine levels, are important markers for assessing renal function and metabolic status, and inflammation reflects the body's inflammatory state and immune response. The model group showed higher levels of all six indicators compared to the other groups (**Figure 2A-F**). While the CA group did not show significant differences from the control group, the model group exhibited substantial changes across all indicators, confirming the successful induction of the HUA model. The results from the negative control group supported the experiment's validity and reliability. Compared to the model group, all doses of 6-O-Caffeoylarbutin showed significant therapeutic benefits, similar to the positive control. In conclusion, these results suggest that 6-O-Caffeoylarbutin can reduce inflammation, decrease tubular interstitial breadth, and im-

prove renal damage and tubular luminal dilation in the HUA model.

*Identification and enrichment analysis of 6-O-Caffeoylarbutin targets*

**Figure 3A** and **3B** show the 2D and 3D structures of 6-O-Caffeoylarbutin. The SEA database predicted 66 potential targets for 6-O-Caffeoylarbutin, the SuperPred database identifies 93 targets, and the STP database suggests 102 targets. To better understand the relationships between these predicted targets, we used jvenn [22] for visualization. A total of 221 union targets and 1 intersection target (TDP1) were identified across the SEA, SuperPred, and STP databases (**Figure 3C**).

The 221 fusion targets of 6-O-Caffeoylarbutin were subjected to GO and KEGG enrichment analyses, with a significance threshold of $P < 0.05$. These fusion-target genes had 1544 GO keywords in total, with 1083 being significant ($P < 0.05$, **Figure 3D**). The target genes are primarily involved in biological processes related to kidney function, including transmembrane transport, kidney development, and responses to external stimuli (**Figure 3D**). Additionally, **Figure 3E** highlights the role of endopeptidase and serine hydrolase activities in metabolic processes critical for uric acid regulation, suggesting that 6-O-Caffeoylarbutin's effects on HUA pathways are partially mediated by these overlapping genes.

*KEGG pathway enrichment*

A total of 119 out of 133 KEGG pathways containing the 6-O-Caffeoylarbutin target genes were significantly enriched ($P < 0.05$). These pathways were primarily were related to biological processes relevant to HUA, including purine metabolism, mTOR signaling, AGE-RAGE signaling, PI3K-Akt signaling, MAPK signaling, and HIF-1 signaling (**Figure 3F**). These findings indicate that 6-O-Caffeoylarbutin may regulate oxidative stress, apoptosis, inflammation, and metabolic processes involved in uric acid homeostasis. Furthermore, **Figure 3G** illustrates the relationships between key pathways, such as the AGE-RAGE signaling pathway, VEGF signaling pathway, PI3K-Akt signaling pathway, MAPK signaling pathway, and purine metabolism, which share overlapping genes involved in the regulation of HUA.

*Identification of 6-O-Caffeoylarbutin targets for HUN treatment and PPI network construction analysis*

The ClinVar, DisGeNET, MalaCards, and Phenolyzer databases identified 76, 196, 62, and 737 potential HUA-RGs, respectively. To visualize the correlation of these HUA-RGs across the databases, jvenn [22] was used. The union of the HUA-RGs from the four databases included 960 genes, with 9 intersection genes, as shown in **Figure 4A**. The DisGeNET, MalaCards, and Phenolyzer databases identified 16, 44, and 599 potential urate nephropathy-related genes (UN-RGs) using the "ureteral nephropathy" keyword, respectively. However, no relevant genes were retrieved from the ClinVar database. Visualization using jvenn [22] showed 656 union UN-RGs and no intersection UN-RGs across the DisGeNET, MalaCards, and Phenolyzer databases (**Figure 4B**). In this study, the intersection of HUA-RGs and UN-RGs was treated as a combined set of uric acid-related genes (UA-RGs). **Figure 4C** demonstrates that the union of HUA-RGs and UN-RGs consists of 1560 genes, with 56 common genes.

The six potential targets of 6-O-Caffeoylarbutin for treating HUN were identified as SLC37A4, XDH, SERPINE1, ALB, SLC28A2, and HPRT1 (**Figure 4D**). The PPI network for these targets is shown in **Figure 4E**, with six targets and eight edges (interaction pairs). The connectivity ranks of these targets were as follows: ALB (4), XDH (4), HPRT1 (3), SERPINE1 (3), SLC28A2 (1), and SLC37A4 (1) (**Figure 4F**), indicating that these are the most likely key targets for 6-O-Caffeoylarbutin in the treatment of HUN.

*Molecular docking and validation analysis*

Molecular docking studies were performed using AutoDockTools software to evaluate the potential of core target compounds for treating HUA (HUN). The docking analysis revealed that 6-O-Caffeoylarbutin formed stable interactions with target proteins at several binding sites across six docking studies. The binding mode analysis showed that the compound predominantly interacted with the target protein through π-π stacking, hydrophobic interactions, and hydrogen bonds, all contributing to enhanced binding stability. Stronger affinity and more stable binding were associated with lower binding energies. The binding energies of

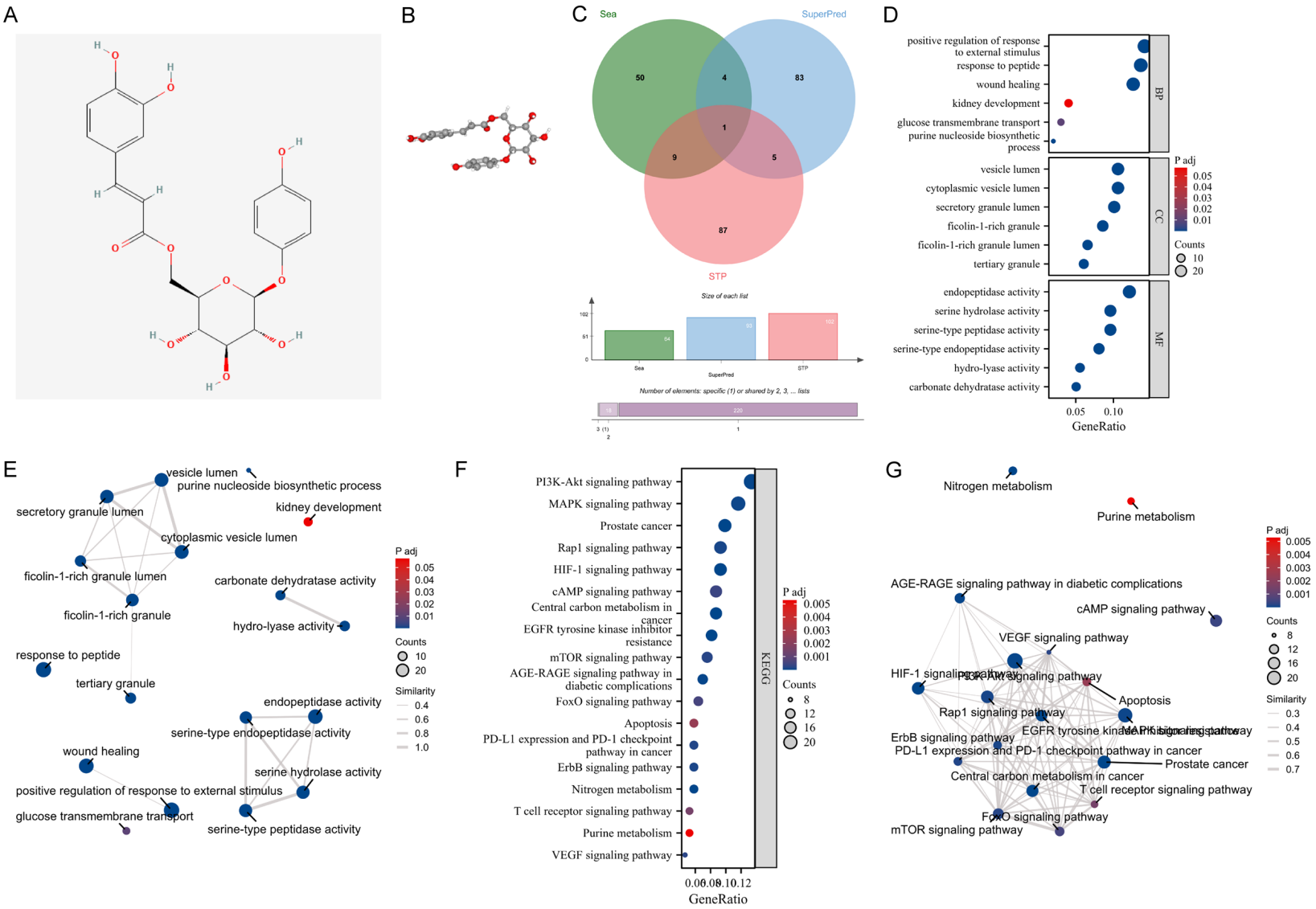


**Figure 3.** Structural and Functional Characterization of 6-O-Caffeoylarbutin Target Genes and Pathways. (A, B) 2D structure (A) and 3D structure (B) of 6-O-Caffeoylarbutin. (C) Venn diagram of predicted target proteins of 6-O-Caffeoylarbutin. (D, F) Bubble chart of Gene Ontology (GO) (D) and Kyoto Encyclopedia of Genes and Genomes (KEGG) (F) enrichment of 6-O-Caffeoylarbutin and target genes, the larger the point, the more targets are enriched. The redder the color, the more significant it is. (E, G) EMAP network diagram of GO (E) and KEGG (G) enrichment of 6-O-Caffeoylarbutin and target genes, the larger the point, the more enriched the target is. The redder the color, the more significant it is. The thicker the line, the higher the similarity.

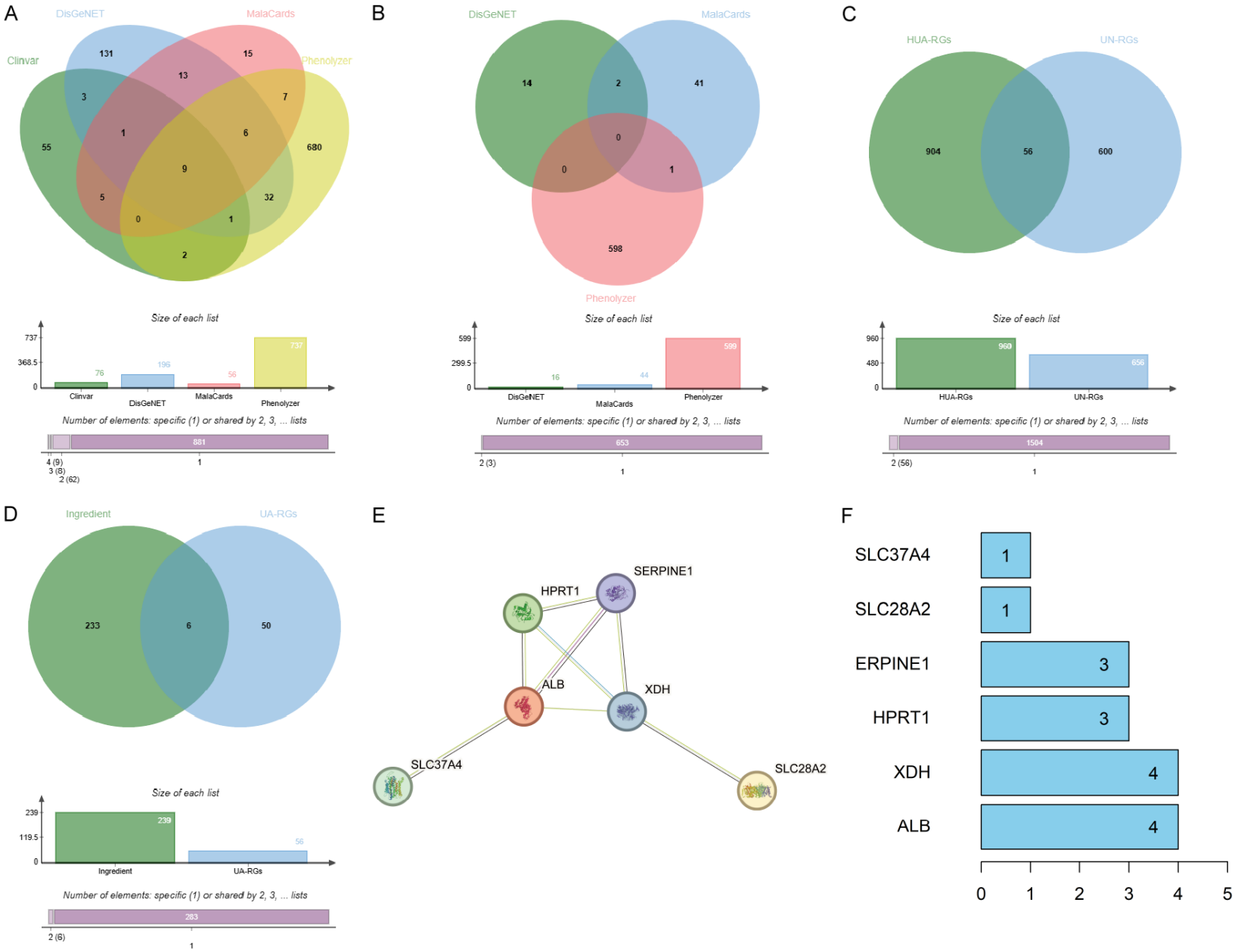
A
DisGeNET
MalaCards
Clinvar
Phenolyzer
131
15
13
3
7
1
6
55
680
9
5
32
0
1
2
Size of each list
737
368.5
0
76
196
56
737
Clinvar
DisGeNET
MalaCards
Phenolyzer
Number of elements: specific (1) or shared by 2, 3, ... lists
881
4 (9)
3 (8)
2 (62)
1
B
DisGeNET
MalaCards
14
2
41
0
0
1
598
Phenolyzer
Size of each list
599
299.5
0
16
44
599
DisGeNET
MalaCards
Phenolyzer
Number of elements: specific (1) or shared by 2, 3, ... lists
653
2 (3)
1
C
HUA-RGs
UN-RGs
904
56
600
Size of each list
960
480
0
960
656
HUA-RGs
UN-RGs
Number of elements: specific (1) or shared by 2, 3, ... lists
1504
2 (56)
1
D
Ingredient
UA-RGs
233
6
50
Size of each list
239
119.5
0
239
56
Ingredient
UA-RGs
Number of elements: specific (1) or shared by 2, 3, ... lists
283
2 (6)
1
E
SERPINE1
HPRT1
ALB
XDH
SLC37A4
SLC28A2
F
SLC37A4
1
SLC28A2
1
ERPINE1
3
HPRT1
3
XDH
4
ALB
4
0
1
2
3
4
5

**Figure 4.** Identification and Network Analysis of Key Genes Targeted by 6-O-Caffeoylarbutin in Hyperuricemia (HUA) Treatment. A. Venn diagram of HUA-RGs. B. Venn diagram of UN-RGs. C. Venn diagram of HUA-RGs and HN-RGs. D. Intersection genes of target genes of HUA-RGs union and 6-O-Caffeoylarbutin union (HUN-RGs). E. Protein-Protein Interaction (PPI) network of genes underlying HUN treatment by 6-O-Caffeoylarbutin, each circle represents a target, and lines of different colors represent different evidences of interactions between targets. F. Target connectivity counts in the PPI network of possible genes for 6-O-Caffeoylarbutin treatment of HUN. The higher the connectivity, the more critical the target is.

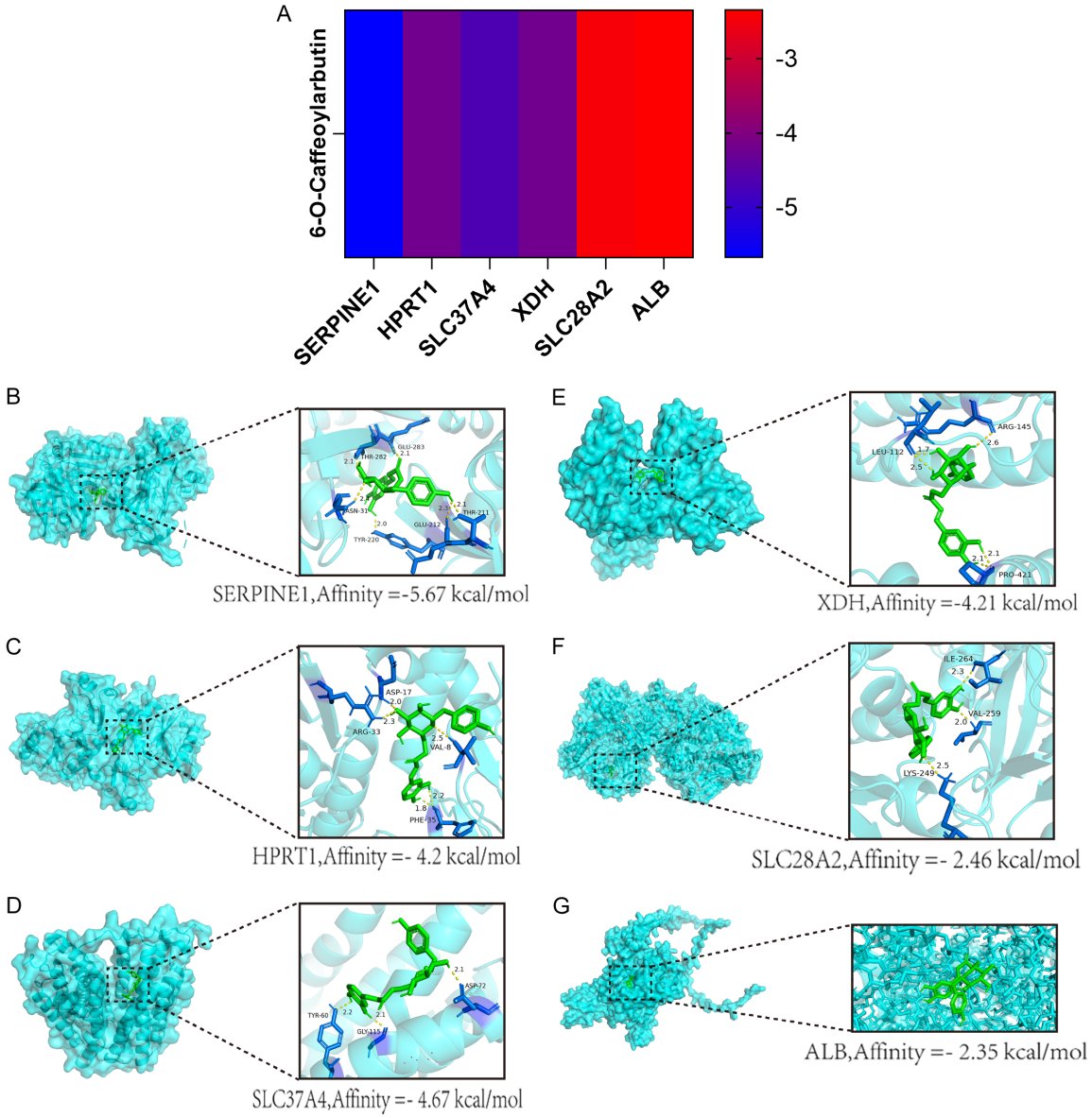


**Figure 5.** Molecular docking visualization. Note: (A) Binding energy heat map. (B) SERPINE1. (C) HPRT1. (D) SLC37A4. (E) XDH. (F) SLC28A2. (G) ALB. For example, B is the molecular docking of 6-O-Caffeoylarbutin and SERPINE1.

all docking studies were less than -2.35 kcal/mol (**Figure 5A-G**), indicating a significant interaction.

The stability of these complexes was further reinforced by the aromatic ring structure's involvement in π-π interactions and the formation of a stable hydrogen bond network between 6-O-Caffeoylarbutin and key amino acid residues. Hydrophobic contacts also played a crucial role in stabilizing the molecular complexes, suggesting that component binding

can occur independently. The six docking types are shown in **Figure 5B-G**, emphasizing the importance of molecular interactions in the design of effective protein inhibitors.

*Effects of 6-O-Caffeoylarbutin on target protein expression in HUN*

According to network pharmacology, 6-O-Caffeoylarbutin targets six proteins for the treatment of HUN. The results indicated that the relative expression of the six target genes in the HUA model group was significantly higher than in the control group. However, except for SLC37A4 and SLC28A2, the 6-O-Caffeoylarbutin treatment group showed a significant decrease in the expression levels of four proteins, especially in the HM-CA3 group, when compared to the model group (**Figure 6A-D**). These findings suggest that 6-O-Caffeoylarbutin plays a significant role in modulating these target proteins, offering a potential novel therapeutic approach for HUN.

## Discussion

The combination of *in vivo* validation and comprehensive network pharmacology analysis demonstrated that 6-O-Caffeoylarbutin exerts therapeutic effects against HUA and renal inflammation through a multi-target mechanism. In a HUA mouse model, our results showed that 6-O-Caffeoylarbutin not only significantly reduces SUA levels but also improves kidney damage and inhibits inflammatory reactions. 6-O-Caffeoylarbutin may exert its pleiotropic effects through six key target proteins - XDH, SERPINE1, HPRT1, SLC37A4, SLC28A2, and ALB - which were identified and confirmed through network pharmacology prediction, molecular docking, and experimental validation.

The HUA mouse model was established using intraperitoneal injection of PO combined with HX gavage. This modeling approach is widely used in HUA research because it closely mimics the clinical features of disorders involving human uric acid metabolism [11, 12]. Previous studies have shown that the PO+HX-induced model typically exhibits elevated SUA levels, renal tissue damage (including inflammatory cell infiltration, tubular dilation, and interstitial edema), and impaired renal function (elevated creatinine and urea nitrogen levels) [4, 12]. The experimental findings in this study align with these previous reports, further demonstrating that 6-O-Caffeoylarbutin can partially restore renal function and dramatically lower SUA levels in HUA mice.

6-O-Caffeoylarbutin exhibits anti-inflammatory properties by inhibiting inflammatory pathways such as NF-κB and MAPK, reducing the release of proinflammatory factors such as IL-1β and TNF-α [8, 23]. The ELISA results in this study further support these findings, showing significant reductions in IL-1β, TNF-α, and IL-6 levels in mice treated with 6-O-Caffeoylarbutin. Additionally, 6-O-Caffeoylarbutin may be safer and better tolerated than benzbromarone, a commonly used clinical medication for reducing uric acid. While benzbromarone effectively increases uric acid excretion, prolonged use has been linked to liver toxicity [5, 24]. In contrast, 6-O-Caffeoylarbutin, as a natural compound, may have fewer adverse side effects, making it a promising candidate for HUA treatment. By targeting multiple important proteins, 6-O-Caffeoylarbutin may offer both kidney protection and uric acid-lowering effects.

Molecular docking studies revealed that 6-O-Caffeoylarbutin interacts stably with six key targets, including XDH, SERPINE1, HPRT1, SLC37A4, SLC28A2, and ALB, with binding energies below -2.35 kcal/mol. These interactions were further confirmed by WB analysis, reinforcing the hypothesis of a multi-target therapeutic mechanism for HUA. XDH, a rate-limiting enzyme in purine metabolism, catalyzes the oxidation of HX and xanthine to uric acid. Under normal physiological conditions, oxidative stress can convert XDH into XOD, which plays a key role in uric acid synthesis [25]. Overactivation of XOD is a major contributor to HUA. Excessive XOD-mediated uric acid production not only increases blood uric acid levels but also exacerbates oxidative stress, further damaging renal tissue [26]. Clinically, uric acid-lowering drugs such as febuxostat and allopurinol target XOD to reduce uric acid synthesis [27]. WB analysis in this study demonstrated that 6-O-Caffeoylarbutin treatment increased XDH expression, suggesting that 6-O-Caffeoylarbutin may primarily reduce uric acid synthesis by stabilizing XDH and preventing its conversion to XOD. Furthermore, 6-O-Caffeoylarbutin may act as a competitive inhibitor of XOD, directly blocking its activity and

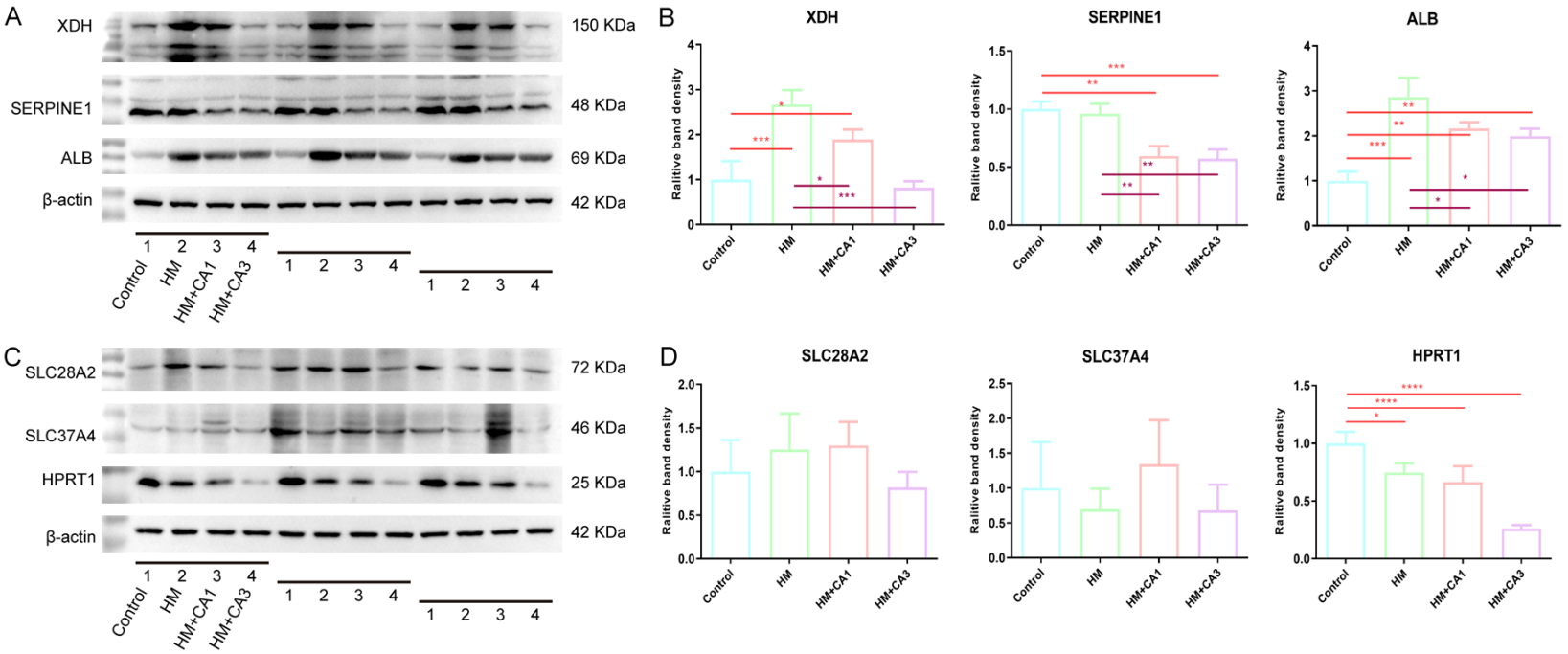


**Figure 6.** Effect of 6-O-Caffeoylarbutin on Protein Expression in HUA Models. A. Representative western blot (WB) images of XDH, SERPINE1, and ALB. B. Quantitative analysis data of XDH, SERPINE1, and ALB are shown (n = 3, *P < 0.05). C. Representative WB images of SLC28A2, SLC37A4, and HPRT1. D. Quantitative analysis data of SLC28A2, SLC37A4, and HPRT1 are shown (mean ± SD, n = 3, *P < 0.05). HM: HUA model. HM-CA1: HUA model plus 1100 mg.kg-1 of 6-O-Caffeoylarbutin. HM-CA3: HUA model plus 1100 mg.kg-1 of 6-O-Caffeoylarbutin.

thereby lowering uric acid production. These findings indicate that 6-O-Caffeoylarbutin, as a natural XOD inhibitor, holds promise for reducing blood uric acid levels.

Plasminogen activator inhibitor-1 (PAI-1), primarily encoded by SERPINE1, is crucial for the fibrinolytic system, coagulation, and inflammatory response. By inhibiting tissue-type and urokinase-type plasminogen activators (tPA/uPA), PAI-1 regulates the balance between thrombosis and fibrinolysis [28]. Studies have shown that patients with HUA have significantly elevated plasma PAI-1 levels, which may contribute to vascular dysfunction, inflammation, and chronic renal injury [29]. 6-O-Caffeoylarbutin decreased SERPINE1 expression, which could mitigate renal damage in HUA by reducing inflammatory and fibrotic responses associated with PAI-1. Therefore, 6-O-Caffeoylarbutin may inhibit SERPINE1, exerting both anti-inflammatory and renal protective effects.

HPRT1 plays a critical role in the purine salvage pathway, facilitating the conversion of HX to inosinic acid and preventing the breakdown of purines into uric acid [30]. Mutations in HPRT1 cause Lesch-Nyhan syndrome, characterized by significantly high uric acid levels [31]. Research has demonstrated that reduced HPRT1 activity exacerbates uric acid accumulation and disrupts purine metabolism. In this study, WB analysis showed that 6-O-Caffeoylarbutin increased HPRT1 expression, which may enhance purine salvage and reduce uric acid production.

SLC37A4 is crucial for energy metabolism and uric acid excretion, as it primarily transports glucose-6-phosphate in the kidneys and liver [32]. Deficiency in SLC37A4 can lead to glycogen storage disease (GSD) [33] and contribute to HUA and renal damage. WB findings from this study showed that 6-O-Caffeoylarbutin increased SLC37A4 expression, potentially enhancing renal function and promoting uric acid excretion by improving glucose metabolism.

SLC28A2 primarily functions in adenosine transport, influencing both adenosine and uric acid metabolism [34]. Low expression of SLC28A2 can lead to adenosine accumulation, which is then converted to uric acid [35]. In this study, WB results showed that 6-O-Caffeoylarbutin upregulated SLC28A2, suggesting that it may reduce uric acid levels by promoting adenosine transport and limiting its breakdown into uric acid.

ALB plays a key role in regulating plasma osmotic pressure, and changes in its levels have been associated with uric acid metabolism [36]. WB analysis in this study indicated that 6-O-Caffeoylarbutin affects ALB regulation, which may contribute to the balance of uric acid metabolism.

Despite these promising findings, this study has several limitations. First, the pharmacologic effects and mechanisms were primarily investigated using a single HUA animal model induced by PO and HX. Future studies should validate these results in other models, such as urate oxidase-knockout mice, which develop spontaneous HUA, to enhance the generalizability of the conclusions. Second, while network pharmacology and molecular docking identified several key targets, the precise regulatory mechanisms - such as whether 6-O-Caffeoylarbutin directly inhibits XOD activity or interacts with other signaling pathways like NF-κB or PI3K-Akt - require further validation using techniques including surface plasmon resonance (SPR), electrophoretic mobility shift assays (EMSA), or gene knockout models. Third, the pharmacokinetic profile, bioavailability, and long-term safety of 6-O-Caffeoylarbutin remain unclear, which are crucial for its development as a therapeutic agent. Future research should focus on addressing these limitations, exploring the structure-activity relationship of 6-O-Caffeoylarbutin derivatives, and translating these preclinical findings into clinical applications.

## Conclusion

This study provides a scientific foundation for the use of 6-O-Caffeoylarbutin for the treatment of HUA and sheds light on its molecular mechanisms. Compared to conventional uric acid-lowering medications, 6-O-Caffeoylarbutin shows multi-target regulatory capabilities, positioning it as a promising novel therapeutic option for HUA. Furthermore, the combination of network pharmacology and experimental research can be applied to investigate the efficacy of other natural compounds, offering a guide for the development of new therapeutic agents.

## Acknowledgements

The authors thank the Experimental Center of Kunming Medical University and the Third People's Hospital of Yunnan Province for their support and assistance. This work was supported by Research Project on Undergraduate Educational and Teaching Reforms in Yunnan Province (JG2023001), the fund for Opening fund project of Yunnan Provincial Key Laboratory of Pharmacology for Natural Products (7012401020107) and First-Class Discipline Team of Kunming Medical University (2024-XKTDTS14).

## Disclosure of conflict of interest

None.

**Address correspondence to:** Baochun Shen, School of Pharmaceutical Sciences and Yunnan Provincial Key Laboratory of Pharmacology for Natural Products, Kunming Medical University, Kunming 650500, Yunnan, China. E-mail: shenbaochun@kmmu.edu.cn

## References

[1] Arrebola JP, Ramos JJ, Bartolomé M, Esteban M, Huetos O, Cañas AI, López-Herranz A, Calvo E, Pérez-Gómez B and Castaño A. Associations of multiple exposures to persistent toxic substances with the risk of hyperuricemia and subclinical uric acid levels in BIOAMBIENT.ES study. Environ Int 2019; 123: 512-521.

[2] Simão AN, Lozovoy MA and Dichi I. The uric acid metabolism pathway as a therapeutic target in hyperuricemia related to metabolic syndrome. Expert Opin Ther Targets 2012; 16: 1175-1187.

[3] Yin X, Huang S, Xiong T and Peng F. Effects of Lactobacillus plantarum NCU1546 fermentation on active components, in vitro uric acid lowering activity and flavor of Lilium. Food Bioscience 2025; 65: 106112.

[4] Wang Z, Li Y, Liao W, Huang J, Liu Y, Li Z and Tang J. Gut microbiota remodeling: a promising therapeutic strategy to confront hyperuricemia and gout. Front Cell Infect Microbiol 2022; 12: 935723.

[5] Strilchuk L, Fogacci F and Cicero AF. Safety and tolerability of available urate-lowering drugs: a critical review. Expert Opin Drug Saf 2019; 18: 261-271.

[6] Suzuki S, Yoshihisa A, Yokokawa T, Kobayashi A, Yamaki T, Kunii H, Nakazato K, Tsuda A, Tsuda T, Ishibashi T, Konno I, Yamaguchi O, Machii H, Nozaki N, Niizeki T, Miyamoto T and Takeishi Y. Comparison between febuxostat and allopurinol uric acid-lowering therapy in patients with chronic heart failure and hyperuricemia: a multicenter randomized controlled trial. J Int Med Res 2021; 49: 3000605211062770.

[7] Zhao T, Sun M, Kong L, Xue Q, Wang Y, Wang Y, Khan A, Cao J and Cheng G. Bioactivity-guided isolation of phytochemicals from vaccinium dunalianum wight and their antioxidant and enzyme inhibitory activities. Molecules 2021; 26: 2075.

[8] Adem Ş, Eyupoglu V, Sarfraz I, Rasul A, Zahoor AF, Ali M, Abdalla M, Ibrahim IM and Elfiky AA. Caffeic acid derivatives (CAFDs) as inhibitors of SARS-CoV-2: CAFDs-based functional foods as a potential alternative approach to combat COVID-19. Phytomedicine 2021; 85: 153310.

[9] Wang YP, Wang YD, Liu YP, Cao JX, Yang ML, Wang YF, Khan A, Zhao TR and Cheng GG. 6'-O-Caffeoylarbutin from Que Zui tea ameliorates acetaminophen-induced liver injury via enhancing antioxidant ability and regulating the PI3K signaling pathway. Food Funct 2022; 13: 5299-5316.

[10] Ma J, Huang J, Hua S, Zhang Y, Zhang Y, Li T, Dong L, Gao Q and Fu X. The ethnopharmacology, phytochemistry and pharmacology of angelica biserrata - a review. J Ethnopharmacol 2019; 231: 152-169.

[11] Ling L, Wei YX, Sun YF, Zhang MJ, Chen J, Luo SY and Xue JW. Effect of androgen on bone metabolism in hyperuricemic rats. Arch Med Sci 2022; 18: 1351-1356.

[12] Xu Z, Sha W, Hou C, Amakye WK, Yao M and Ren J. Comparison of 3 hyperuricemia mouse models and evaluation of food-derived anti-hyperuricemia compound with spontaneous hyperuricemia mouse model. Biochem Biophys Res Commun 2022; 630: 41-49.

[13] Shi P, Zheng B, Cao Y, Niu G and Guo Q. Study on the mechanism of Trichosanthes kirilowii Maxim. against COPD based on serum chemical composition analysis, network pharmacology, and experimental study. Phytomedicine 2025; 140: 156533.

[14] Povodovski L, Makaryan V, Sabo P, Dicken Y, Herman A, Emmanuel R and Dale DC. Safe and efficient engraftment of CRISPR-based ELANE mono-allelic knocked out HSCs in mice: evidence for a novel treatment for ELANE neutropenia. Blood 2021; 138: 3122.

[15] Landrum MJ, Lee JM, Benson M, Brown GR, Chao C, Chitipiralla S, Gu B, Hart J, Hoffman D, Jang W, Karapetyan K, Katz K, Liu C, Maddipatla Z, Malheiro A, McDaniel K, Ovetsky M, Riley G, Zhou G, Holmes JB, Kattman BL and Maglott DR. ClinVar: improving access to variant

interpretations and supporting evidence. Nucleic Acids Res 2018; 46: D1062-D1067.
[16] Piñero J, Bravo À, Queralt-Rosinach N, Gutiérrez-Sacristán A, Deu-Pons J, Centeno E, García-García J, Sanz F and Furlong LI. DisGeNET: a comprehensive platform integrating information on human disease-associated genes and variants. Nucleic Acids Res 2017; 45: D833-d839.
[17] Rappaport N, Twik M, Plaschkes I, Nudel R, Iny Stein T, Levitt J, Gershoni M, Morrey CP, Safran M and Lancet D. MalaCards: an amalgamated human disease compendium with diverse clinical and genetic annotation and structured search. Nucleic Acids Res 2017; 45: D877-D887.
[18] Yang H, Robinson PN and Wang K. Phenolyzer: phenotype-based prioritization of candidate genes for human diseases. Nat Methods 2015; 12: 841-843.
[19] Wu T, Hu E, Xu S, Chen M, Guo P, Dai Z, Feng T, Zhou L, Tang W, Zhan L, Fu X, Liu S, Bo X and Yu G. clusterProfiler 4.0: a universal enrichment tool for interpreting omics data. Innovation (Camb) 2021; 2: 100141.
[20] Waterhouse A, Bertoni M, Bienert S, Studer G, Tauriello G, Gumienny R, Heer FT, de Beer TAP, Rempfer C, Bordoli L, Lepore R and Schwede T. SWISS-MODEL: homology modelling of protein structures and complexes. Nucleic Acids Res 2018; 46: W296-W303.
[21] Jargieło W, Małysiak-Mrozek B and Mrozek D. PIF - A Java library for finding atomic interactions and extracting geometric features supporting the analysis of protein structures. Methods 2022; 205: 63-72.
[22] Bardou P, Mariette J, Escudié F, Djemiel C and Klopp C. jvenn: an interactive Venn diagram viewer. BMC Bioinformatics 2014; 15: 293.
[23] Liu Y, Zheng K, Wang H, Liu H, Zheng K, Zhang J, Han L, Tu S and Wang Y. Natural bioactive compounds: emerging therapies for hyperuricemia. Am J Chin Med 2024; 52: 1863-1885.
[24] Lin P, Chen Z and Lin J. Therapeutic drugs of gout: the progress in target selection. Int J Rheum Dis 2024; 27: e15022.
[25] Chen-Xu M, Yokose C, Rai SK, Pillinger MH and Choi HK. Contemporary prevalence of gout and hyperuricemia in the united states and decadal trends: the national health and nutrition examination survey, 2007-2016. Arthritis Rheumatol 2019; 71: 991-999.
[26] Battelli MG, Polito L and Bolognesi A. Xanthine oxidoreductase in atherosclerosis pathogenesis: not only oxidative stress. Atherosclerosis 2014; 237: 562-567.
[27] Kuo CF, Grainge MJ, Mallen C, Zhang W and Doherty M. Rising burden of gout in the UK but continuing suboptimal management: a nationwide population study. Ann Rheum Dis 2015; 74: 661-667.
[28] Pascart T and Lioté F. Gout: state of the art after a decade of developments. Rheumatology (Oxford) 2019; 58: 27-44.
[29] Dalbeth N, Gosling AL, Gaffo A and Abhishek A. Gout. Lancet 2021; 397: 1843-1855.
[30] Khanna D, Fitzgerald JD, Khanna PP, Bae S, Singh MK, Neogi T, Pillinger MH, Merill J, Lee S, Prakash S, Kaldas M, Gogia M, Perez-Ruiz F, Taylor W, Lioté F, Choi H, Singh JA, Dalbeth N, Kaplan S, Niyyar V, Jones D, Yarows SA, Roessler B, Kerr G, King C, Levy G, Furst DE, Edwards NL, Mandell B, Schumacher HR, Robbins M, Wenger N and Terkeltaub R. 2012 American College of Rheumatology guidelines for management of gout. Part 1: systematic nonpharmacologic and pharmacologic therapeutic approaches to hyperuricemia. Arthritis Care Res (Hoboken) 2012; 64: 1431-1446.
[31] Richette P, Doherty M, Pascual E, Barskova V, Becce F, Castañeda-Sanabria J, Coyfish M, Guillo S, Jansen TL, Janssens H, Lioté F, Mallen C, Nuki G, Perez-Ruiz F, Pimentao J, Punzi L, Pywell T, So A, Tausche AK, Uhlig T, Zavada J, Zhang W, Tubach F and Bardin T. 2016 updated EULAR evidence-based recommendations for the management of gout. Ann Rheum Dis 2017; 76: 29-42.
[32] Stamp LK and Dalbeth N. Prevention and treatment of gout. Nat Rev Rheumatol 2019; 15: 68-70.
[33] Luzzatto L, Nannelli C and Notaro R. Glucose-6-phosphate dehydrogenase deficiency. Hematol Oncol Clin North Am 2016; 30: 373-393.
[34] Perez-Ruiz F and Dalbeth N. Gout. Rheum Dis Clin North Am 2019; 45: 583-591.
[35] Kuo CF, Grainge MJ, See LC, Yu KH, Luo SF, Zhang W and Doherty M. Epidemiology and management of gout in Taiwan: a nationwide population study. Arthritis Res Ther 2015; 17: 13.
[36] Dehlin M, Jacobsson L and Roddy E. Global epidemiology of gout: prevalence, incidence, treatment patterns and risk factors. Nat Rev Rheumatol 2020; 16: 380-390.